

Nonergodic Subdiffusion from Transient Interactions with Heterogeneous Partners

C. Charalambous,¹ G. Muñoz-Gil,¹ A. Celi,¹ M.F. Garcia-Parajo,^{1,2}
M. Lewenstein,^{1,2} C. Manzo,^{1,*} and M.A. García-March^{1,†}

¹*ICFO-Institut de Ciències Fotòniques, The Barcelona Institute of
Science and Technology, 08860 Castelldefels (Barcelona), Spain*
²*ICREA - Pg. Lluís Companys 23, 08010 Barcelona, Spain*

Spatiotemporal disorder has been recently associated to the occurrence of anomalous nonergodic diffusion of molecular components in biological systems, but the underlying microscopic mechanism is still unclear. We introduce a model in which a particle performs continuous Brownian motion with changes of diffusion coefficients induced by transient molecular interactions with diffusive binding partners. In spite of the exponential distribution of waiting times, the model shows subdiffusion and nonergodicity similar to the heavy-tailed continuous time random walk. The dependence of these properties on the density of binding partners is analyzed and discussed. Our work provide an experimentally-testable microscopic model to investigate the nature of nonergodicity in disordered media.

Introduction. Advances in fluorescence-based videomicroscopy have recently enabled tracking the movement of small particles and individual molecules with nanometer precision in living cells [1]. These experiments have allowed the evaluation of several observables which characterize the dynamics of a variety of biomolecules. Remarkably, in many biological systems, they have revealed that the mean squared displacement (MSD) shows a nonlinear growth in time

$$\text{MSD}(t) \sim t^\alpha \quad \text{with } 0 < \alpha < 1, \quad (1)$$

and thus deviates from Brownian motion ($\alpha = 1$). Furthermore, the detailed analysis of the particle trajectories has shown that some processes characterized by *anomalous* diffusion also exhibit differences between ensemble and time averaged observables, such as the mean squared displacement itself [2–7]. This feature, known as weak-ergodicity breaking [8], reflects the physical nature of specific stochastic mechanisms, for which time averages are random and thus irreproducible in spite of the large statistics. These properties are captured by a number of nonstationary stochastic processes [9], such as the heavy-tailed continuous time random walk (CTRW) [10], or heterogeneous diffusion processes [9].

All these models postulate the presence of some form of kinetic heterogeneity in the system, e.g. a nonconstant diffusion coefficient, which causes the nonergodic behavior. Recent measurements reporting on the variation of diffusion coefficient in space or time [12–14], sometimes associated with anomalous and nonergodic diffusion [7], justify these assumptions phenomenologically. However, some questions remain unanswered: What causes such kinetic heterogeneity at the microscopic level? Which is the associated mechanism leading to nonergodic anomalous diffusion? Experimental evidences have recently shown that specific interactions between molecules diffusing on the cell membrane can temporarily modify their diffusive behavior [15] but there is lack of a microscopic model encompassing a mechanistic link between interactions and

nonergodic subdiffusion.

In this paper, we introduce a model of ordinary CTRW in which anomalous diffusion and nonergodicity arise as a consequence of transient molecular interactions with a population of diffusing binding partners. In our simple physical picture, the Brownian motion of a random walker called *prey*, is temporarily modified upon interactions with a set of random walkers called *hunters*: as a consequence of the interaction, the motion of the prey is altered by a factor randomly drawn from a distribution with a power law tail. A particular case of this general scenario is provided by a distribution obtained considering that the diffusivity is the sum of several squared Gaussian random variables arising out of many microscopic degrees of freedom [22]. We also consider a case in which interactions slow down the diffusion of the prey, in order to reflect the experimental scenarios in which interactions produce the transient binding to other diffusing molecules, thus leading to the formation of higher order species (homo- or hetero-dimers or oligomers). The broad diffusivity distribution of our model is in agreement with several experimental reports [18]. In addition, it accounts for the presence of heterogeneity in interaction products (i.e. formation of nanoclusters with a varying number of molecules and thus different diffusivities) as well as in interacting partners (i.e. interactions with a pool of chemically different species with different diffusivity).

As for the heavy-tail CTRW, also in this case the ergodicity breaking is generated by energetic disorder due to transient chemical binding [10]. However, in the model discussed here, the waiting times are always drawn from an exponential distribution, therefore even while interacting, the prey always perform Brownian motion. A crucial aspect of this model is that we explicitly introduce a physical mechanism (i.e., transient interactions) causing the change of diffusivity. Moreover, even though the prey experiences the disorder only for a limited amount of time (i.e., upon interaction), this is sufficient to generate anomalous diffusion and nonergodicity even in the

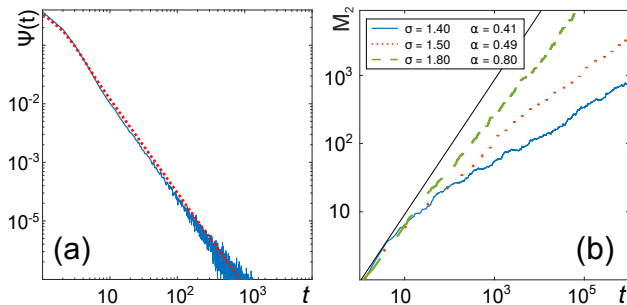


FIG. 1. (a) Analytical (dashed line) *vs* numerically-calculated (solid line) waiting time distribution for $\sigma = 1.6$. (b) Ensemble mean squared displacement calculated for different values of σ , showing the subdiffusive behavior in the asymptotic regime and the agreement of the exponent α with the theoretical predicted values. The black solid thin line indicates the exponent $\alpha = 1$. These results correspond to $N = 8$ hunters and $L = 20$ sites.

dilute limit. The occurrence of such interactions can be experimentally verified, e.g. using multicolor single particle tracking experiments [15]. This sets a great advantage over models with diffusion coefficient varying in space [16] or time [17]. After describing the model, we calculate the effective waiting time distribution and the ensemble-averaged MSD (eMSD), discussing the origin of subdiffusivity. Next, we present the results of numerical simulations, for which we also calculate the time-averaged MSD (tMSD) and the ergodicity breaking (EB) parameter. Last, we discuss potential applications and address future developments of the model.

The model. We consider a random walker (*prey*) interacting with a system of N independent random walkers (*hunters*) moving in d -dimensional regular lattices with $m = L^d$ sites and $d = 1, 2$. Periodic boundary conditions ensure constant hunters' density in time. Both types of walker perform a CTRW with waiting times drawn from an exponential distribution $\psi_0(t) = (1/\tau) \exp[-t/\tau]$. The interaction between the prey and the hunters is devised as follows: when the prey coincides at a lattice site with at least one of the hunters, the waiting time for the next step is drawn from a distribution $\psi_\kappa(t) = (1/\kappa\tau) \exp[-t/\kappa\tau]$, with κ stochastically chosen from any probability distribution $P_\kappa(\kappa)$, such that as $\kappa \rightarrow \infty$

$$P_\kappa(\kappa) \approx \kappa^{-\sigma} \quad \text{with } \sigma > 1, \quad (2)$$

and with $P_\kappa(\kappa)$ decaying rapidly to 0 for small κ .

Alternatively, we can formulate a similar model by assigning a different value of κ to every hunter with the same probability as in Eq. (2). In this case, every hunter maintains the same κ until it leaves the lattice, and assumes a new value at reentering. Since the probability that the prey reencounters the same hunter is negligibly small, a different value of κ is sampled at every interaction, thus establishing the equivalence between both

realizations of the model.

The probability for the prey to perform n steps with waiting times t_i in a time $t = \sum_{i=1}^n t_i$ is

$$\psi_n(t) = \int_0^t \dots \int_0^t \psi(t_1) \dots \psi(t_n) \delta\left(t - \sum_{i=1}^n t_i\right) dt_1 \dots dt_n,$$

where the waiting time distribution $\psi(t)$ must account for the cases of encountering ($\psi(t) = \psi_\kappa$) or not a hunter ($\psi(t) = \psi_0$). If p_{NH} is the probability of not hitting a hunter, and $p_{\text{H}} = 1 - p_{\text{NH}}$ its complement, we can then write

$$\psi(t) = p_{\text{NH}} \psi_0(t) + p_{\text{H}} \int_0^\infty P_\kappa(\kappa) \psi_\kappa(t) d\kappa. \quad (3)$$

Since the hunters have constant density, perform independent random walks, and can simultaneously occupy the same site, p_{NH} results to be constant in time and can be expressed as $p_{\text{NH}} = \left(\frac{m-1}{m}\right)^N$.

We first consider a distribution $P_\kappa(\kappa)$ given by a Gamma distribution:

$$P_\kappa(\kappa) = A \kappa^{-\sigma} e^{-\frac{\kappa}{\tau}}, \quad (4)$$

with $A = \frac{b^{\sigma-1}}{\Gamma[\sigma-1]}$, which has the same functional dependence of the distribution (χ^2) one obtains by considering the inverse rate (i.e. the diffusivity) as the sum of several squared Gaussian random variables arising out of many microscopic degrees of freedom [22].

By performing a transformation of variable $D = 1/\kappa$, we can solve the integral in Eq. (3)

$$\frac{A}{\tau} \int_0^\infty D^{\sigma-1} e^{-Db} e^{-\frac{Dt}{\tau}} dD = \frac{b^{\sigma-1}}{\sigma} \left(b + \frac{t}{\tau}\right)^{-\sigma}, \quad (5)$$

thus the waiting time distribution shows a heavy-tail for $1 < \sigma < 2$.

Another possible scenario is represented by the situation in which interactions with an hunter can only slow down the diffusion of the prey, thus corresponding to a distribution with a minimum value for κ , such as

$$P_\kappa(\kappa) = (\sigma - 1) \cdot \theta[\kappa - 1] \kappa^{-\sigma} \quad (6)$$

where $\theta[\cdot]$ represents the Heaviside step function.

In this case, the integral in Eq. (3) gives

$$\frac{1}{\tau} \int_0^1 D^{\sigma-1} e^{-\frac{Dt}{\tau}} dD = \frac{1}{\tau} \left(\frac{t}{\tau}\right)^{-\sigma} (\Gamma[\sigma] - \Gamma[\sigma, t/\tau]), \quad (7)$$

where $\Gamma[\sigma, t/\tau] = \int_{t/\tau}^\infty r^{\sigma-1} \exp[-r] dr$ is the upper incomplete Gamma function.

This function converges exponentially to zero as $t \rightarrow \infty$. Therefore, in the long-time limit, it has the same behavior as the first term of Eq. (3) and they can be both neglected.

It follows that the waiting time distribution for $t \rightarrow \infty$ can be approximated as

$$\psi(t) \approx p_H \frac{\Gamma[\sigma]}{\tau} \left(\frac{t}{\tau}\right)^{-\sigma} = \frac{1}{\tau} \left(\frac{t}{\tau}\right)^{-\sigma}, \quad (8)$$

where $(\frac{t}{\tau})^{\sigma-1} = p_H \Gamma[\sigma]$.

In order to prove that this distribution leads to a subdiffusive behavior, we calculate the eMSD $M_2(t) = \langle x^2(t) \rangle$, where x is the distance of the prey from its initial position and $\langle \cdot \rangle$ represents ensemble average over multiple trajectories. Although the following calculations refer to the rate distribution in Eq. (6), qualitatively similar results are obtained for any distribution as in Eq. (2).

The Laplace transform of the eMSD, $M_2(s)$, can be obtained as

$$M_2(s) = \frac{\psi(s)}{s[1-\psi(s)]} \langle l^2 \rangle. \quad (9)$$

Taking the normalized form of $\psi(t)$ (i.e. $\psi(s \rightarrow 0) = 1$) for $\psi(t)$ given by the asymptotic formula Eq. (8), a Tauberian theorem [19] permits to obtain $\psi(s) \propto (1 - \tilde{\tau}^\alpha s^\alpha)$, with $\alpha = \sigma - 1$. Then, the eMSD is $M_2(s) = \frac{1 - \tilde{\tau}^\alpha s^\alpha}{\tilde{\tau}^\alpha s^{\alpha+1} \Gamma}$, which for large t (i.e. small s) and for $0 \leq \alpha \leq 1$ gives $M_2(s) \approx \frac{1}{\tilde{\tau}^\alpha s^{\alpha+1}}$. Finally, its inverse Laplace transform (L^{-1}) provides

$$M_2(t) = L^{-1}[M_2(s)](t) \approx \frac{1}{\Gamma(\sigma)} \left(\frac{t}{\tau}\right)^\alpha, \quad (10)$$

where $M_2(s) \approx \tilde{\tau}^{-\alpha} s^{-(\alpha+1)}$.

It is worth to remind here that the coefficient $\tilde{\tau}$ depends through p_H on both the number of hunters N and of sites m ,

$$\tilde{\tau} = \tilde{\tau}(N, m) \propto \left[1 - \left(\frac{m-1}{m}\right)^N\right]^{\frac{1}{\alpha}}. \quad (11)$$

For dilute systems (large m), one can approximate the probability of hitting a hunter as $p_H \approx N/m$. The dependence of the eMSD on N and m through p_H can be verified both numerically and experimentally, thus providing a relevant experimental observable to test the model.

The presence of nonergodicity implies that the time averaged mean square displacement (tMSD)

$$\overline{\delta^2}(t, t_{\text{lag}}) = \frac{\int_0^{t-t_{\text{lag}}} [x(t' + t_{\text{lag}}) - x(t')]^2 dt'}{t - t_{\text{lag}}},$$

remain random variables for different trajectories at all time lags. To give a quantitative measure of the nonergodicity, the ergodicity breaking (EB) parameter was introduced as [20]

$$\text{EB} = \lim_{t \rightarrow \infty} \frac{\langle (\overline{\delta^2})^2 \rangle - \langle \overline{\delta^2} \rangle^2}{\langle \overline{\delta^2} \rangle^2}. \quad (12)$$

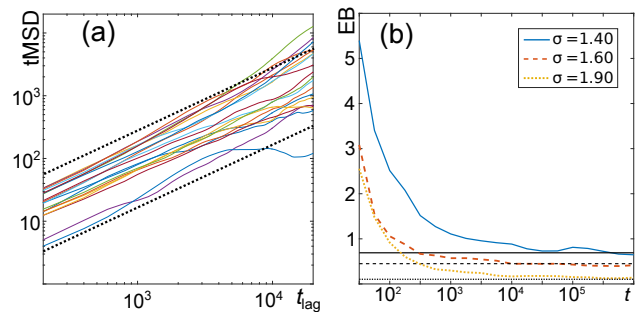


FIG. 2. (a) Time averaged mean squared displacement obtained for 20 representative prey trajectories with $\sigma = 1.8$, $N = 6$ and $L = 20$. The curves show a linear behavior but large scattering of their amplitude at all time lags, as expected for weak nonergodic behavior. Dashed lines correspond to linear behavior and are meant as a guide to the eye. (b) Ergodicity breaking (EB) parameter calculated as a function of total time of measurement t for several values of σ and $N = 10$. At large t all the curves asymptotically tend to the value predicted by Eq. (13) [horizontal black lines, line types correspond to different σ], as expected for a nonergodic behavior. As σ is reduced, the system departs more from ergodicity and the EB shows larger asymptotic value.

In the case of an ergodic process the EB parameter should be 0, while $\text{EB} > 0$ indicates nonergodicity. For a heavy tailed CTRW, where the waiting times are distributed according to a power law, the EB parameter is given by [20]

$$\text{EB} = \frac{2\Gamma^2[\sigma]}{\Gamma[2\sigma - 1]} - 1. \quad (13)$$

This result also applies to the case described here, as one can rewrite Eq. (8) as $\psi(t) \sim t^{-(1+\alpha)}/|\Gamma(-\alpha)|$.

Numerical results. We simulated the master equation associated to the system of a prey and N independent hunters by means of a Monte Carlo method in 1D. We take $\tau = 1$ in all calculations, so that, we consider *long times* as t larger than 1 in three or four orders of magnitude. The numerically-calculated waiting time distribution is represented in Fig. 1 (a) together with the analytical prediction $\psi(t)$ in Eq. (3), showing an excellent agreement. In panel (b) of this figure, we also plot the curves obtained by the calculation of eMSD, showing the asymptotic subdiffusive behavior $\sim t^\alpha$ for $1 < \sigma < 2$, as predicted by the theory.

Consistently with the model prediction, the representative tMSD curves shown in Fig. 2(a) display a linear behavior but large scattering of their values at all time lags, confirming that time averages are random and thus lead to nonergodicity. To quantitatively corroborate this observation, we calculated EB with Eq. (12). In Fig. 2(b), we show that the value of EB converges to the value theoretically predicted by Eq. (13) for $1 < \sigma < 2$. As σ is decreased from 2 towards 1 the system becomes more nonergodic (larger EB).

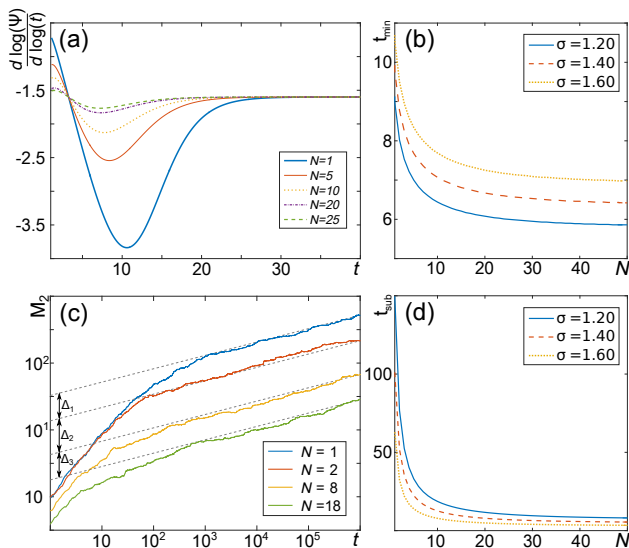


FIG. 3. (a) Logarithmic derivative of the distribution of waiting times as in Eq. (3) for $\sigma = 1.6$ and different values of the number of hunters. For large t , the derivative tends to the expected value of $-\sigma$ [corresponding to the exponent of Fig. 1(a) at long times]. (b) Time t_{\min} at which the minima of the curve in panel (a) are reached, as a function of the number of hunters N . The larger the number of hunters, the quicker the logarithmic derivative of the waiting time distribution tends to its asymptotic value σ (shorter t_{\min}). (c) eMSD for different number of hunters and $\sigma = 1.2$. The long-time power-law behavior of the eMSD with exponent $\alpha = 0.2$, is independent of the number of hunters. In the asymptotic regime, curves obtained for different numbers of hunters are separated by a distance Δ . (d) Analytically-calculated time t_{sub} at which the subdiffusive behavior occurs as a function of N .

Finally, we obtain that the long time properties of the system, like the exponent α quantifying the subdiffusive behavior and the value of the EB parameter, do not depend on the density of hunters N/L . However, as the density of hunters N/L is increased, the weight p_H also increases, thus the second term of the probability distribution Eq. (3) becomes dominant with respect to the first one at shorter times. To exemplify this behavior, in Fig. 3(a) we plot the logarithmic derivative of the distribution of waiting times Eq. (3), for different number of hunters. All the curves cross at a value equal to σ , which can be analytically calculated to occur at $t = \sigma\tau$. In addition, all the curves show a qualitatively similar behavior, decreasing to reach a minimum and then increasing towards the asymptotic value σ . In Fig. 3(b), we plot the time t_{\min} at which this minimum is reached as a function of the number of hunters, showing that - as N increases - the time at which the curve approaches its asymptotic value decreases. In Fig. 3(c) we also plot the eMSD for different numbers of hunters and $\sigma = 1.2$. In all cases, the curves asymptotically tend to a power law with exponent $\alpha \simeq 0.2$. Equations (10) and (11) set the

dependence of the eMSD on the number of hunters: once reached the asymptotic behavior, the distance between two curves obtained for N_i and N_j hunters respectively is given by $\Delta = \log(p_H(N_j)/p_H(N_i))$. In the dilute limit ($m \gg 1$), this expression reduces to $\Delta = \log(N_j/N_i)$. We found good agreement between this analytical prediction and the numerically calculated Δ . Finally, due to the dependence of eMSD on p_H , one can give a lower bound for the time required for the subdiffusive behavior to emerge, t_{sub} . This lower bound can be obtained as the time at which the logarithm of the long-time power-law behavior [Eq. (10)] and of the short-time linear behavior of the eMSD intersect, giving $t_{\text{sub}} = \frac{10^{1-\alpha}}{p_H \Gamma(\sigma)^2}$. From the plot of t_{sub} in Fig. 3(d), one can note that while its qualitative behavior is similar to t_{\min} [Fig. 3(b)], t_{sub} is always larger than t_{\min} as expected. Remarkably, for the same number of hunters, t_{sub} and t_{\min} have inverse dependence to $\Gamma(\sigma)$. Increasing σ , the heavy tailed part of the waiting time distribution Eq. (3) becomes dominant at larger times, while subdiffusion emerges at shorter times.

Conclusions. The model discussed in this paper proposes a mechanistic explanation for the nonergodic subdiffusion observed in several biological systems [2–7], based on the occurrence of specific, transient interactions with a heterogeneous population of interacting partners. The model displays many similarities with the long-time behavior of the heavy-tail CTRW [10] and the patch model [17]. However, there are crucial differences that, in our opinion, make our model extremely suitable for the interpretation of experimental data of molecular diffusion on the cell membrane. First, in contrast to the heavy-tail CTRW model, the model does not require particle immobilization. The waiting time distribution - and thus the distribution of interaction time between the prey and a hunter - is exponential as expected for a Markov process. Therefore, our model allows to reproduce nonergodic behavior without requiring to postulate time-dependent effects to justify power law distributions for the interactions or trapping time [21]. For the CTRW with heavy-tail waiting time distribution, the presence of “annealed” or “quenched” disorder produces different diffusion laws in $d = 1, 2$. This is a consequence of the fact that - when the rate at a given lattice site is constant (“quenched”) - correlations arise between successive arrival times [11]. Our model can also be formulated in two versions, one in which a hunter picks a random rate every time it encounters a prey, and one in which each hunter has a constant rate. However, in both realizations of our model, the sampling of transition rates - and therefore the disorder - is highly dynamical as it occurs through the hunter-prey interaction mechanism and thus does not induce any correlations. Therefore, in both cases we obtain the same scaling law as for the “annealed” trap model, to which our model exactly converges to in the high density limit ($N \rightarrow \infty$).

Our model also shows similarities with the long-time behavior of the time-annealed patch model [17] for the value of the exponent $\gamma = 1$. However, in the patch model, the disorder is ubiquitous in space and/or time and the random walker continuously undergoes changes of diffusivity. In our case, in contrast the prey typically diffuses in a Brownian fashion with constant D , except for the local changes of diffusivity experienced for a limited amount of time upon interactions with the hunter. Therefore, we show that anomalous diffusion and nonergodicity can emerge even in presence of partial disorder (small N).

The proposed framework relies on the assumption of a broad distribution of the diffusion rates (or diffusion coefficients) of the interacting partners. We consider this assumption rather reasonable since the hunters in our model might represent different chemical species and on the basis of broad diffusivity distributions reported for chemically identical cellular components [18]. Moreover, our general requirements for the distribution of rates include the particular case in which the diffusivity is the sum of several squared Gaussian random variables, e.g. due to the presence of a large number of degrees of freedom [22].

Last, the model offers the possibility of being experimentally tested, e.g. by means of multicolor single particle tracking techniques, thus allowing to distinguish its occurrence from other theoretical frameworks. Moreover, it allows to estimate microscopic parameters of the system under investigation - such as the average density of hunters - from the eMSD curve and the timescale of onset of subdiffusion.

Acknowledgements. We acknowledge discussions with Gerald John Lapeyre, Jr. and useful comments to the arXiv version from Eli Barkai. This work was supported by Fundació Cellex, Generalitat de Catalunya (Grant No. 2009 SGR 597 and 2014 SGR 874), the European Commission [FP7-ICT-2011-7, Grant No. 288263; SIQS (FP7-ICT-2011-9 No 600645); EU STREP QUIC (H2020-FETPROACT-2014 No 641122); EQuaM (FP7/2007 – 2013 Grant No 323714)]; the HFSP (Grant RGP0027/2012), OSYRIS (ERC-2013-AdG Grant No 339106) and the Spanish Ministry of Science and Innovation (Grants FOQUS FIS2013-46768-P and MAT2011-22887). Financial support from the Spanish Ministry of Economy and Competitiveness, through the “Severo Ochoa” Programme for Centres of Excellence in R&D (SEV-2015-0522) is acknowledged.

* carlo.manzo@icfo.es

† miguel.garcia-march@icfo.es

- [1] C. Manzo, and M.F. Garcia-Parajo, Rep. Progr. Phys. **78**, 124601 (2015).
- [2] I. Golding, and E. C. Cox, Phys. Rev. Lett. **96**, 098102 (2006).
- [3] I. Bronstein, Y. Israel, E. Kepten, S. Mai, Y. Shav-Tal, E. Barkai, and Y. Garini, Phys. Rev. Lett. **103**, 018102 (2009).
- [4] J.-H. Jeon, V. Tejedor, S. Burov, E. Barkai, C. Selhuber-Unkel, K. Berg-Sørensen, L. Oddershede, and R. Metzler, Phys. Rev. Lett. **106**, 048103 (2011).
- [5] A. V. Weigel, B. Simon, M. M. Tamkun, and D. Krapf, Proc. Natl. Acad. Sci. USA **108**, 6438 (2011).
- [6] S. M. A. Tabei, S. Burov, H. Y. Kim, A. Kuznetsov, T. Huynh, J. Jureller, L. H. Philipson, A. R. Dinner, and N. F. Scherer, Proc. Natl. Acad. Sci. USA **110**, 4911 (2013).
- [7] C. Manzo, J.A. Torreno-Pina, P. Massignan, G.J. Lapeyre, Jr., M. Lewenstein, and M.F. Garcia-Parajo Phys. Rev. X **5**, 011021 (2015).
- [8] J.-P. Bouchaud, J. Phys. I, **2**, 1705 (1992).
- [9] R. Metzler, J.-H. Jeon, A.G. Cherstvy, and E. Barkai Phys. Chem. Chem. Phys., **16**, 24128 (2014).
- [10] H. Scher, and E.W. Montroll, Phys. Rev. B **12**, 2455 (1975).
- [11] J.-P. Bouchaud, and A. Georges, Phys. Rep. **195**, 127–293 (1990).
- [12] J.-B. Masson, P. Dionne, C. Salvatico, M. Renner, C.G. Specht, A. Triller, and M. Dahan, Biophys. J. **106** 74 (2014).
- [13] S. Manley, J.M. Gillette, G. H. Patterson, H. Shroff, H. F. Hess, E. Betzig, and J. Lippincott-Schwartz, Nat. Methods **5**, 155 (2008).
- [14] P. J. Cutler, M.D. Malik, S. Liu, J. M. Byars, D. S. Lidke, and K. A. Lidke, PLoS One **8**, e64320 (2013).
- [15] J. A. Torreno-Pina, C. Manzo, M.F. Garcia-Parajo J. Phys. D: Applied Physics **49**, 104002 (2016).
- [16] A. G. Cherstvy, and R. Metzler, Phys. Chem. Chem. Phys. **15**, 20220 (2013).
- [17] P. Massignan, C. Manzo, J. A. Torreno-Pina, M.F. Garcia-Parajo, M. Lewenstein, and G.J. Lapeyre, Jr., Phys. Rev. Lett. **112**, 150603 (2014).
- [18] M. J. Saxton, Biophys. J. **72**, 1744–1753 (1997).
- [19] J. Klafter, and I. M. Sokolov, First Steps in Random Walks (Oxford University Press, Oxford, 2011).
- [20] Y. He, S. Burov, R. Metzler, and E. Barkai, Phys. Rev. Lett. **101**, 058101 (2008).
- [21] A.V. Weigel, M.M. Tamkun, and D. Krapf Proc. Nat. Acad. Sci. USA **110** E4591–E4600 (2013).
- [22] C. Beck, E. G. D. Cohen, H. L. Swinney Phys. Rev. E, **72** 056133 (2005).